The Range Increase of Adaptive Versus Phased Arrays in Mobile Radio Systems

Jack H. Winters, *Fellow, IEEE,* and Michael J. Gans

***Abstract*—In this paper, we compare the increase in range with multiple-antenna base stations using adaptive array combining to that of phased array combining. With adaptive arrays, the received signals at the antennas are combined to maximize signal-to-interference-plus-noise ratio (SINR) rather than only form a directed beam. Although more complex to implement, adaptive arrays have the advantage of higher diversity gain and antenna gain that is not limited by the scattering angle of the multipath at the mobile. Here, we use computer simulation to illustrate these advantages for range increase in both narrow-band and spread-spectrum mobile radio systems. For example, our results show that for a 3° scattering angle (typical in urban areas), a 100-element array base station can increase the range 2.8 and 5.5-fold with a phased array and an adaptive array, respectively. Also, for this scattering angle, the range increase of a phased array with 100 elements can be achieved by an adaptive array with only ten elements.**

***Index Terms*—Adaptive arrays, mobile communications, multipath channels, phased arrays.**

I. Introduction

MULTIPLE antennas at the base station can provide increased received signal gain and, thus, range in mobile radio systems. Two approaches for combining the received signals are the phased array, which creates an antenna beam directed at the mobile, and the adaptive array, which maximizes signal-to-interference-plus-noise ratio (SINR). Here, we compare the range increase of phased arrays to that of the more complex adaptive array technique for both narrow-band and spread-spectrum systems.

Previous papers have studied the increase in gain with phased arrays [1]–[6]. With phased arrays, the signals received by each antenna are weighted and combined to create a beam in the direction of the mobile. The same performance can also be achieved by sectorized antennas, whereby a different antenna is used to form each beam. As the number of antennas increases, the received signal gain (range) increases proportionally to the number of antennas, but only until the beamwidth of the array is equal to that of the angle of multipath scattering around the mobile. Beyond that point, the increased gain of more antennas is reduced by the loss of power from scatterers outside the beamwidth. The range can even be reduced with narrower beamwidths because the resulting reduction in delay spread can cause a loss of diversity gain in systems using equalization, e.g., in spread-spectrum systems using a RAKE receiver.

This limitation in range increase can be overcome by the use of adaptive arrays [5]–[9]. With adaptive arrays, the signals received by each antenna are weighted and combined to maximize the output SINR. Although the most widely studied advantage of adaptive arrays is interference suppression [7]–[10], maximizing SINR also forms an antenna pattern matched to the wavefront (which is not a plane wave for nonzero scattering angle) and therefore provides a range increase that is not limited by the scattering angle. In addition, adaptive arrays can provide higher diversity gain than phased arrays, since all the receive antennas can be used for diversity combining. Thus, for a given number of antennas, adaptive arrays can provide greater range, or require fewer antennas to achieve a given range.

In this paper, we describe the limitations of phased arrays for range increase and describe how these limitations can be overcome using adaptive arrays.[1] We use computer simulation to illustrate our results for the range increase in both narrow-band and spread-spectrum mobile radio systems. For example, our results show that for a 3° scattering angle, a 100-element array base station can increase the range 2.8 and 5.5-fold with a phased array and an adaptive array, respectively. Also, for this scattering angle, the range increase of a phased array with 100 elements can be achieved by an adaptive array with only ten elements.

In Section II, we discuss the theoretical performance of phased and adaptive arrays. We present a mobile radio system model and illustrate the performance results by computer simulation in Section III.

II. Description of Phased and Adaptive Arrays

A. Phased Array

Fig. 1 shows a block diagram of a phased array with omnidirectional elements linearly spaced at $\lambda/2$, where λ is the signal wavelength. The signals received by the antennas are weighted and combined to form a beam at angle ϕ, i.e., the signal at the ith antenna is phase shifted by $\pi(i-1)\sin\phi, i = 1, \cdots M$.

For the mobile radio base station, the antenna beam should be narrow in elevation and the antenna characteristics should be independent of azimuth. A narrow elevation angle can be

Manuscript received September 19, 1994; revised July 19, 1998.
J. H. Winters is with AT&T Labs–Research, Red Bank, NJ 07701 USA.
M. J. Gans is with Lucent Bell Labs, Holmdel, NJ 07733 USA.
Publisher Item Identifier S 0018-9545(99)01067-1.

[1] Note that we consider range increase as a convenient way to express the effect of gain increase, and it also corresponds to a decrease in required number of base stations to cover a given area.

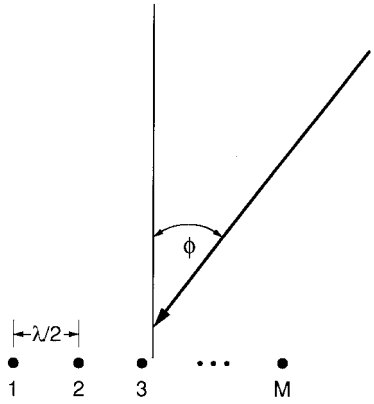

Fig. 1. Linear phased array with omnidirectional elements linearly spaced at $\lambda/2$.

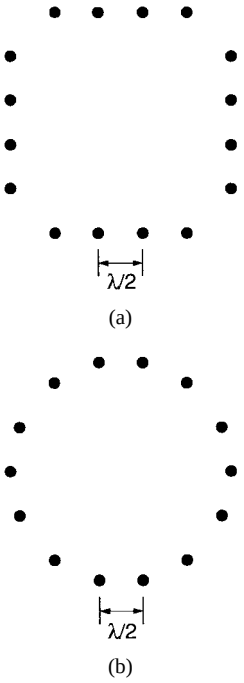

Fig. 2. (a) Array with linear elements on four panels in a square and (b) with elements on a cylinder.

created by using a vertical array of antenna elements for each horizontal element. The azimuth dependence can be reduced by placing the linear elements on four panels in a square, as shown in Fig. 2(a) [11]. However, a cylindrical array, as shown in Fig. 2(b), is usually used to create azimuth independence. Each antenna element is typically spaced at $\lambda/2$, since smaller spacing reduces gain by creating a wider beamwidth with increased mutual coupling, while wider spacing can also reduce gain by decreasing the beamwidth and creating grating lobes, i.e., gain in directions other than the desired angle-of-arrival. The effect of antenna spacing on mutual coupling is studied in Appendix A.

To create a beam in a given direction, the signals from the antenna elements are cophased, based on a plane wave arrival. Since to reduce mutual coupling between elements, each element should have higher gain in the direction pointing away from the center of the cylinder (see Appendix A), the signals should also be weighted by the voltage gain in the given direction to maximize signal-to-noise ratio (SNR) in the array output. These weighted signals are summed to generate the array output, with the output SNR for a beam with direction ϕ given by

$$S/N(\phi) = \frac{\left|\sum_{i=1}^{M} s_{\mathrm{rec}_i} \cdot s_i^*(\phi)\right|^2}{\sum_{i=1}^{M} |s_i(\phi)|^2} \tag{1}$$

where s_{rec_i} is the complex received signal voltage at antenna i, $s_i(\phi)$ is the expected (based on antenna location) antenna voltage gain and phase (relative to the other antennas) for a signal arriving from angle ϕ, and the superscript $*$ denotes complex conjugate.

The weights can be implemented at radio frequency (RF) by different cable lengths for the fixed phase offsets and fixed attenuators for the amplitude weighting. The weighted signals for each beam are then combined, with a separate combiner and signal for each beam. For each mobile radio user, the receiver then selects the beam output with the largest power to use for signal demodulation. However, this technique can require a large amount of hardware, including amplifiers, with large M, but the complexity can be reduced somewhat by combining only a portion of the antenna outputs—the signals from the antennas with the largest gain in a given direction—for each beam. Alternatively, the signal from each antenna can be brought to baseband and analog–digital (A/D) converted, with the combining done in software. Although this method is similar to adaptive array processing, with the phased array the combining software needs to determine only one parameter, the angle-of-arrival ϕ (which changes slowly with time), for each mobile radio user.

The same performance as the phased array can be achieved by using sectorized antennas, i.e., separate antennas for each beam, as is currently done at many mobile radio base stations. However, to create uniform coverage using sectorized antennas or phased arrays with predetermined (fixed) beams, overlapping beams should be used. (This is also useful for obtaining diversity—see below.) This doubles the number of antennas (with sectorized antennas) or the combining hardware (with phased arrays with fixed beams) without increasing the gain.

Arrays increase the range by providing additional received signal gain due to two factors—antenna gain and diversity gain. With an M-element phased array and a point source, the antenna gain is M, neglecting mutual coupling (see Appendix A). The range increase is the gain raised to the inverse of the propagation loss exponent γ, typically a fourth power loss. Thus, with a point source, the range increase due to the antenna gain of an M-element array is $M^{1/\gamma}$.

However, signal scattering around the mobile means that the signal received at the base station cannot always be considered as coming from a point source. As shown in Fig. 3, with scattering the signal arrives from a range of angles, called the scattering angle. Typically, the mobile signal is scattered mainly by objects within 1000 ft of the mobile,

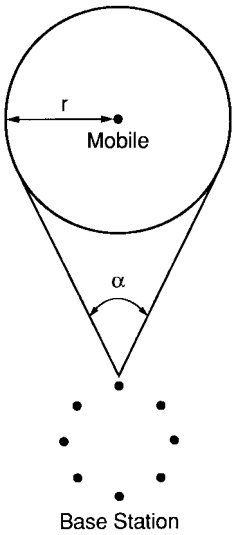

Fig. 3. Mobile radio environment with scattering around the mobile, where all signals from a mobile arrive within a scattering angle α.

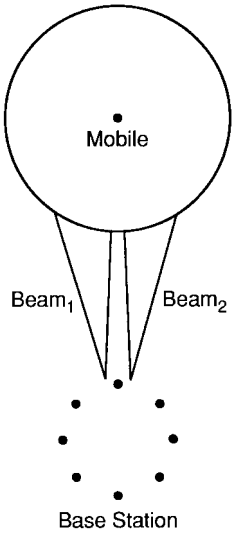

Fig. 4. Cylindrical array using of angle diversity.

but this distance can vary widely, e.g., with reflections off mountains [12]. Furthermore, this scattering angle increases with decreasing base-station height. Measured results for rural areas with 130-ft antenna heights show scattering angles of only a few tenths of a degree, while suburban and urban areas have much larger scattering angles [13]. Measured results in urban areas of Tokyo, Japan, for ranges up to 7 km [14], show a 3° scattering angle at a 50-m antenna height, increasing to 360° at a 1-m height (as on the mobile). In addition, digital mobile radio systems in North America (IS-136) and Europe (GSM) are designed to handle delay spreads up to 41 and 16 μs, respectively, which, with an 8-mi cell radius, correspond to scattering angles of 52° and 21°, respectively. Also, these scattering angles are for 900-MHz mobile radio systems, while at 2 GHz the range is reduced by about 50% (from the Hata model [15], for an antenna height of 50 m at the base station and 1 m at the mobile, medium–small city, and 8-mi cell radius), corresponding to a two-fold scattering angle increase. We expect that microcells will have even larger scattering angles because of the lower antenna height. Here, we do not consider what the likely distribution of scattering angles will be for any given system, but show results obtained for a wide range of scattering angles.

Since receive signal power is lost when the beamwidth, which is approximately $360^\circ/M$ (for a cylindrical array), is less than the scattering angle, the signal gain will be less than M in the phased array with large enough M. For example, for a uniform distribution of power within a scattering angle of α degrees, the maximum signal gain is given by an array with $M = 360/\alpha$ elements. Additional elements increase the antenna gain, but the power lost outside the beam reduces the signal gain by the same amount (under the uniform power distribution assumption). Thus, with phased arrays the signal gain, and the corresponding range increase, is limited.

The other factor for receive signal gain is the diversity gain. Multipath fading results in a higher average output SNR required to achieve a given average receiver performance (e.g., BER in digital systems) than without fading. The fading in the output signal can be reduced by using multiple receive antennas and combining the received signals. We define diversity gain as the improvement in link margin beyond the factor of M for array gain. For example, for a 10^{-2} BER averaged over Rayleigh fading with coherent detection of PSK, a 9.5-dB higher average output SNR is required than without fading. Two antennas provide up to a 5.4-dB diversity gain, while 3, 4, and 6 antennas provide up to 6.8, 7.6, and 8.3 dB, respectively, with maximal ratio combining. Thus, six antennas can provide within 1.2 dB of the maximum diversity gain (i.e., the 9.5-dB gain achieved when the fading is eliminated). However, to achieve the full diversity gain, the fading at the antennas must be nearly independent. This requires that the spacing between antennas is at least the distance such that the beamwidth of an antenna with this aperture is approximately the scattering angle. For example, a spacing of 10–20λ is used for the typical scattering angle of a few degrees [12], [14], [16].

For a cylindrical phased array, such an antenna spacing between elements is impractical and would create numerous grating lobes without providing the antenna gain commensurate with the diameter of the array (or providing diversity gain). However, when the beamwidth of the array is comparable to the scattering angle (i.e., the total array aperture size corresponds to a beamwidth given by the scattering angle), different beams can cover part of the same scattering angle and thereby angle diversity can be used [4], [13], as shown in Fig. 4. For the square array, another set of flat arrays could be spaced 10–20λ apart on each side to provide diversity, as shown in Fig. 5. Note that this is not practical with cylindrical arrays, as the arrays would partially block each other. Similarly, to provide diversity with sectorized antennas, a separate set of antennas can be spaced 10–20λ apart (as is used today) with overlapping sectors to provide more uniform coverage over all azimuth angles. In all cases, though, diversity gain requires additional hardware. To minimize the added cost, usually only dual diversity with selection combining is considered. Note that for the example case of a 10^{-2} BER,

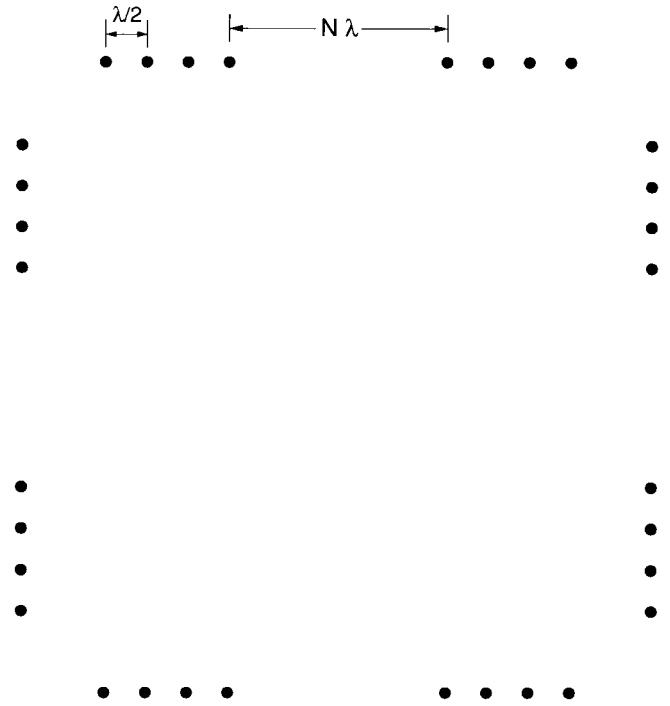

Fig. 5. Square array using space diversity.

selection diversity with two antennas provides only about 3.9 dB of the maximum-possible 9.5-dB diversity gain (which is also 1.5 dB less than maximal ratio combining with two antennas).

Frequency-selective fading due to delay spread can also be used to provide diversity by using equalization [9] in narrow-band systems, or a RAKE receiver in spread-spectrum systems [17]. In this case, the diversity gain of additional antennas is reduced. For example, a three-finger RAKE is used in the IS-95 CDMA system (three fingers on the downlink, but four fingers on the uplink). With received signal energy uniformly distributed over three code symbol periods (2.4 μs), maximal ratio combining of the three fingers provides three-fold diversity, or a 6.8-dB diversity gain at a 10^{-2} BER, and dual antenna diversity provides up to 1.5 dB (the overall combining is equivalent to six-branch maximal ratio combining) of the remaining 2.7-dB maximum diversity gain. Note, however, that, compared to a narrow-band receiver, one finger of this CDMA receiver is 4.8 dB lower in signal power, i.e., the RAKE receiver does not give any increase in average SNR (antenna gain). Finally, note that beamwidths smaller than the scattering angle can reduce the delay spread, and therefore the diversity gain, in systems with phased arrays.

B. Adaptive Array

With an adaptive array, the received signals are combined to maximize the output SINR. Thus, the array can null interference in narrow-band systems[2] (as discussed below), but here we consider only the increase in range due to higher antenna gain. Without interference, the output SNR of an M-element adaptive array is given by

$$S/N = \sum_{i=1}^{M} |s_{\mathrm{rec}_i}|^2. \tag{2}$$

Although (2) is simpler than the SNR equation for the phased array (1), the adaptive array is more complex to implement because the weights are not fixed, but depend on the received signals. Thus, variable gains and phase shifters are needed for each signal on every antenna. These can be implemented in hardware at RF or IF, or in software at baseband. For the software implementation, the signals from each antenna can also be digitized using block processing.

Another complication is the need to acquire and track the weights. As compared to the phased array where the beam or the weights only need to track the angle of the mobile, the adaptive array weights must track the rapid fading of the signal. Algorithms to generate the weights include the constant modulus algorithm (CMA) [18], least-mean-squared (LMS) algorithm [19], and the direct matrix inversion (DMI) algorithm [19]. It should be noted, though, that when interference is not a concern, i.e., when range increase is the issue as in this paper, simpler techniques may be possible for determining the weights.

With the adaptive array, though, the array pattern is matched to the multipath wavefront. That is, there is no antenna gain limitation due to multipath scattering angle, as with phased arrays, and an M-fold diversity gain can also be obtained. Achieving this diversity gain requires adequate antenna spacing however. With a base-station array oriented broadside to a small angle, α degrees, of scatterers around the mobile and with power arriving uniformly at the base from within α, the magnitude of the correlation coefficient between two array elements spaced x wavelengths apart is approximately [see also [14], which approximates the envelope correlation $\rho_e(x)$ by the square of the complex phasor correlation $|\rho(x)|^2$]

$$|\rho(x)| \approx \frac{\sin(\pi^2 \alpha x/180)}{(\pi^2 \alpha x/180)}. \tag{3}$$

Thus, an antenna spacing of $(360°/\pi\alpha)(\lambda/2)$ is required for independent fading at each antenna, but spacings of about half of this still give low-enough fading correlation (<0.7) that nearly the full diversity gain can be achieved. However, even with a spacing of $(360°/(\pi\alpha))(\lambda/4)$, the required array size can be too large. For example, a 3° scattering angle requires a 10-ft antenna spacing at 900 MHz, and, thus, in particular, a 100-element cylindrical array would require a 330-ft diameter. However, since only a few-fold diversity is needed to obtain most of the maximum diversity gain, an array with a diameter of a few times the required antenna spacing (20–30 ft in the above example) should obtain almost all the maximum-possible diversity gain.

Finally, we note that, although not studied in this paper, the adaptive array can also suppress interference. With the narrow beams of large arrays, the number of interferers is greatly reduced in both narrow-band and spread-spectrum systems. Since an M-element array can eliminate N interferers with an $M-N$ diversity gain, large arrays can eliminate any significant

[2] For spread-spectrum systems, nulling of all strong interferers is generally not possible since the number of interferers is typically much greater than the number of antennas.

interference with little loss of diversity or antenna gain. Thus, these arrays can not only greatly increase the range when there is little interference, but they can also be used for future expansion by permitting the capacity to be greatly increased without increasing the number of base stations.

III. Results

A. Model

To verify and illustrate the above conclusions, we used Monte Carlo simulation with the following model (see Fig. 3). We considered transmission from a mobile to a base station. The multipath model consisted of 20 scatterers uniformly distributed in a circular area of radius r around the mobile. These scatterers had equal transmitted power, with a fourth law power loss from each scatterer to the base station. The phase of each multipath reflection at each antenna was determined from the path length. Received power variation due to shadow fading was not considered. The base-station array was a cylindrical array of M equally spaced cardioid antennas [20], with each antenna pointing out from the center of the array, and one element at 0°. The mobile was at 90°. Note that for $M = 2$, the mobile at 90° results in equal gain from the two antennas, while with a mobile at 0° only one antenna has nonzero gain. Thus, for $M = 2$, the results depend strongly on the angle of the mobile (i.e., dual diversity at 90° versus no diversity at 0°). However, for $M \geq 4$, the effect of angle is negligible, and therefore this angle was fixed at 90°. We considered spacings between elements of $\lambda/2$ or greater, and therefore neglected the effect of mutual coupling (see Appendix A).

With the phased array, the weights were set to generate a beam that was pointed directly at the mobile. From (A-8) and (A-10), these weights are given by

$$s_i^*(90^\circ) = \sqrt{2}\cos\left\{\frac{\pi}{4}[\sin(2\pi(i-1)/M) - 1]\right\} \cdot e^{-j(2\pi r/\lambda)\sin(2\pi(i-1)/M)}, \qquad i = 1, \cdots, M \quad (4)$$

and the SNR is then given by (1). With the adaptive array, the weights are $s_{\text{rec}_i}^*, i = 1, \cdots, M$ and the SNR is given by (2). We consider coherent detection of phase-shift-keyed (PSK) signals, for which the BER is given by

$$\text{BER} = \tfrac{1}{2}\,\text{erfc}(\sqrt{S/N}). \quad (5)$$

We used Monte Carlo simulation to determine the BER averaged over 10 000 cases. Note that the BER depends on the ratio of transmit power to receive noise power. This ratio was adjusted to obtain a 10^{-2} average BER for the baseline case of an omnidirectional transmit antenna with the mobile at a given range and scattering radius. With this ratio and the scattering angle fixed, we generated results for the M-element phased and adaptive arrays, increasing the range until the BER exceeded 10^{-2}, thus giving the range increase. All the following results for range increase and diversity gain are referenced to 10^{-2} average BER.

Note that the increase in range is not strongly dependent on the modulation and detection technique considered, but will vary significantly with the power loss exponent and the BER. Specifically, the range increase will be greater than we show in the next section if the power loss exponent is less than four or the required BER is less than 10^{-2}.

We considered both the low data rate case (no delay spread) and the delay spread case. For the delay spread case, the signal delay for each scattered signal depends on the distance from the mobile to the scatterer plus the distance from the scatterer to each base-station antenna.

For the spread-spectrum system with delay spread, we studied the use of a three-finger RAKE receiver for both the phased and adaptive arrays. To simulate the RAKE receiver, the computer program first convolved the delayed impulse of each scatterer with the spread-spectrum correlation function given by

$$f(t) = \begin{cases} 1 - \dfrac{|t_d - t - 0.8|}{0.8}, & \text{for } |t_d - t| \leq 0.8\ \mu\text{s} \\ 0, & \text{elsewhere} \end{cases} \quad (6)$$

where t_d is the time delay corresponding to the distance from the center of the base station to the mobile. The responses from the 20 scatterers were then summed to obtain the signal at each antenna. These signals were weighted and combined by the phased array weights or the adaptive array weights $(s_{\text{rec}_i}^*, i = 1, \cdots, M)$. Note that the adaptive array weights vary as a function of delay. We then determined the three largest peaks in the output response that were separated by integer multiples of the code rate and combined these three signals to maximize the output SNR. That is, these three peaks were cophased and weighted by their signal amplitudes before combining. For the phased array, we considered three different models. In the first model, we considered a single beam pointed at the mobile, i.e., the phased array weights as given in (4). Thus, our model corresponds to phased array combining with a RAKE receiver after the combiner, followed by maximal ratio combining of the RAKE output. To model the IS-95 CDMA system with a phased array, we also considered a RAKE receiver on each antenna, followed by phased array combining of the RAKE outputs, with the beam direction optimized for each delay [rather than set to 90° as in (4)]. Thus, a separate beam was formed for each of the RAKE fingers. Finally, we modified the second model to consider the beam direction optimized over M different, equally spaced angles, which models sectorized antennas. For the adaptive array, our model corresponds to a RAKE receiver on each antenna branch, with adaptive array combining of the antenna signals followed by adaptive array combining of the three highest output peaks, with the receiver timing optimized to maximize the output SNR.

For the no delay spread case, in our simulations we used a 40 000-ft range as the baseline case, with the scattering radius given by the required scattering angle. However, our results can be generalized to any range, as they depend only on the scattering angle and not the absolute values of the range and scattering radius. Therefore, in the next section, we present our results only in terms of the normalized range. Similarly, although we generated results for a one foot wavelength, our results can be generalized to any wavelength. Therefore, our results on antenna spacings are only in terms of λ. Also, for the delay spread case, our simulations used a 1.25-Mbps data rate (as in the IS-95 CDMA system). The scattering radius was

set to 1200 ft (which is typical in mobile radio in suburban and urban areas) which results in a delay spread of three symbols. This radius was chosen because, as shown in the next section, this is the minimum delay spread for which the maximum diversity gain is achieved with the three-finger RAKE receiver. Thus, the scattering radius was chosen to maximize the RAKE diversity gain as well as the effect of a narrow beamwidth on the performance. Again, our results do not depend on the absolute values of the range and scattering radius and are therefore presented in terms of normalized range and scattering angle.

Finally, note that by keeping the scattering radius constant as we increase the range (which would be typical in mobile radio), the scattering angle decreases. For example, a 10° scattering angle with the baseline case is only about 3° with a three-fold range increase. With fixed scattering radius, the predicted range increase discussed in the previous section must therefore be modified. It was noted before that, for a given scattering angle α, the maximum gain is $360/\alpha$, and therefore the maximum range R, normalized to the omnidirectional-antenna range R_0, is given by

$$\frac{R}{R_0} = \left(\frac{360}{\alpha}\right)^{1/4}. \tag{7}$$

But since the scattering radius is kept constant, the scattering angle at range R is less than the baseline scattering angle α_0 at R_0, specifically

$$\alpha = \alpha_0\left(\frac{R_0}{R}\right). \tag{8}$$

Therefore, from (7) and (8), the maximum range increase is given by

$$\frac{R}{R_0} = \left(\frac{360}{\alpha_0}\right)^{1/3} \tag{9}$$

[with the corresponding $M = (360/\alpha_0)^{1/3}$]. This increase is greater than the maximum range increase of $(360/\alpha)^{1/4}$ for the fixed scattering angle case, e.g., the range increase is 4.9 for $\alpha_0 = 3°$ versus 3.3 for $\alpha = 3°$.

B. Results for Range Increase

Fig. 6 shows the normalized maximum range versus the number of antenna elements for phased and adaptive arrays with $\lambda/2$ antenna spacing, neglecting the delay spread. Results are shown for different fixed scattering radii, with the scattering angle for the baseline case of one antenna element given. We also show the theoretical range due to the antenna gain $(M^{1/4})$ without diversity, and due to antenna gain and M-fold diversity. Also, the predicted maximum range with phased arrays is shown.

With the phased array, the range is shown to be limited to the predicted range limitation. However, the range improvement is degraded due to the scattering angle for M less than the theoretical value corresponding to the range limitation, and it requires many times more antennas to actually reach this limitation. For example, with a 20° scattering angle, the predicted range limitation is 2.6, corresponding to 46 antennas, but with 46 antennas the range is only 2.3. Note that at a range

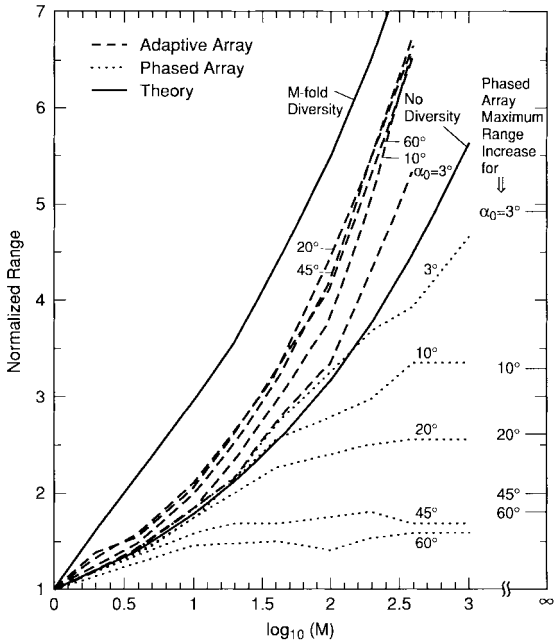

Fig. 6. Normalized maximum range versus the number of antenna elements for phased and adaptive arrays with $\lambda/2$ antenna spacing, neglecting the delay spread.

of 2.6, the scattering angle is reduced to about 8° for the 20° baseline curve.

For the adaptive array, the range exceeds the no-diversity theoretical range for all scattering angles, due to antenna diversity. The diversity gain increases with the scattering angle and M, as expected. However, the diversity gain does not increase for scattering angles greater than about 20°. Thus, because the adaptive array has greater range with increased scattering angle, the difference between the adaptive and phased array increases dramatically with scattering angle.

Next consider the effect of antenna spacing. With the phased array, our results show that the range does not increase with wider spacing, and, in fact, the range decreases if the spacing is wide enough. With the adaptive array, the range increases with antenna spacing, up to that corresponding to the maximum diversity gain. Fig. 7 shows the increase in range with spacing for $M = 2$, 10, and 100 and baseline scattering angles of 3°, 10°, and 20°. Theoretical results for the range with maximum diversity gain are also shown. With baseline scattering angles of 10° or more, the maximum range can be achieved with a spacing of about 10λ. Note that a baseline scattering angle of 10° corresponds to scattering angles of 6.2°, 3.4°, and 1.8° at the maximum range with $M = 2$, 10, and 100, respectively.

Consider the extreme example of a very large array. For a baseline scattering angle of 3°, with 100 elements a spacing of 10λ achieves a 5.15-range increase versus the maximum 5.46, even though the scattering angle at this range is only 0.58° (the array diameter would be 350 ft at 900 MHz and 160 ft at 2 GHz). Thus, with large arrays the antenna spacing can be much less than that required with two antennas to achieve nearly the full diversity gain. As a further example, a 100-element array increases the range about 2.8 times with a phased array and a scattering angle at the maximum range of 3° (about an 8.4°

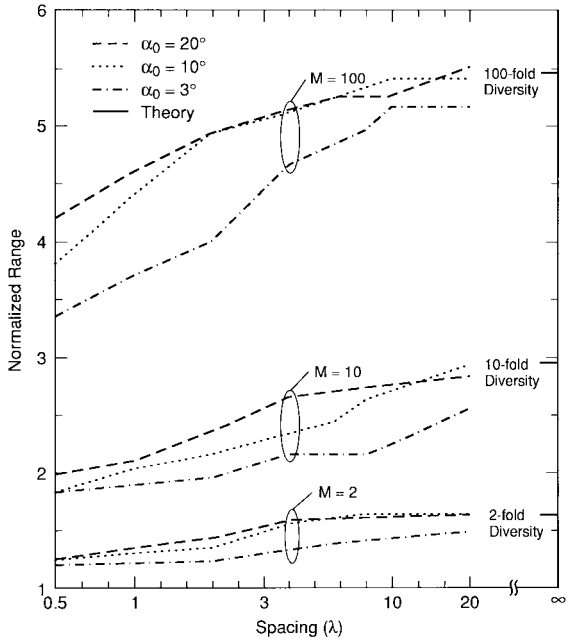

Fig. 7. Increase in range of adaptive arrays with antenna spacing for $M = 2$, 10, and 100 and baseline scattering angles of 3°, 10°, and 20°, neglecting the delay spread.

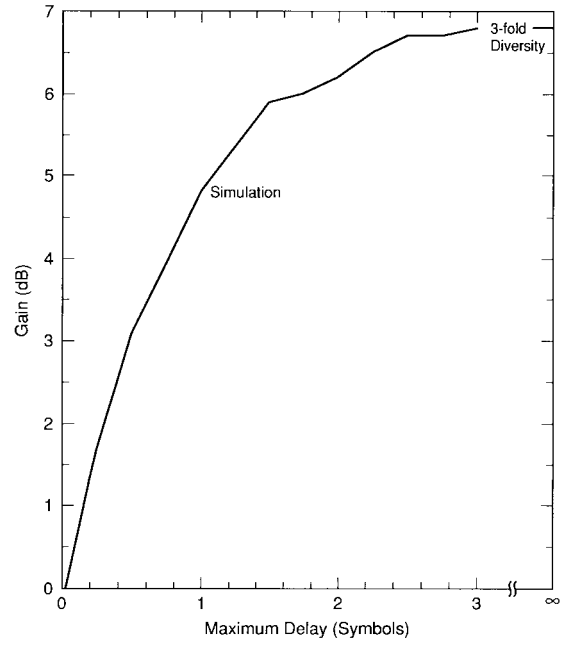

Fig. 8. Diversity gain versus the maximum delay spread for a three-finger RAKE with a single antenna at the base station.

baseline scattering angle) versus 5.5 times for an adaptive array with 10λ antenna spacing. Also, for this scattering angle, the range increase of a phased array with 100 elements can be achieved by an adaptive array with only ten elements.

For the delay spread case with the RAKE receiver, let us first consider the effect of the scattering radius on the diversity gain of the RAKE receiver. Fig. 8 shows the diversity gain versus the maximum delay spread for a three-finger RAKE with a single antenna at the base station. For our model, the maximum delay spread is given by twice the scattering

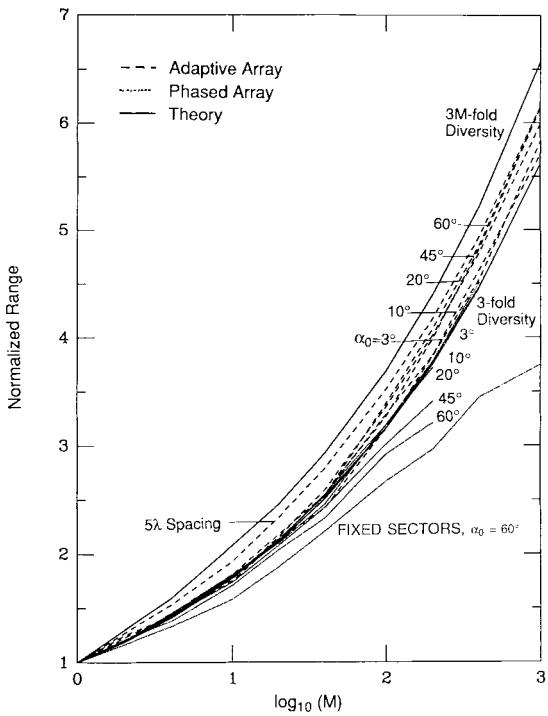

Fig. 9. Normalized maximum range versus the number of antenna elements for phased and adaptive arrays with $\lambda/2$ antenna spacing and a three-finger RAKE receiver.

radius in symbol periods. That is, the minimum delay is given by the delay from the mobile to the base station, while the maximum delay is given by a scatterer at the far edge of the scattering radius along the line between the mobile to the base station. The maximum delay is therefore the propagation time corresponding to twice the scattering radius.

The diversity gain is seen in Fig. 8 to be within 0.1 dB of the maximum possible diversity gain (three-fold diversity) for scattering radii corresponding to delay spreads of three symbols or greater. Therefore, in our simulations, we set the scattering radius to three symbols. Note that with our model, the maximum delay spread does not decrease with the beamwidth of the array because the maximum delay variation is along the line between the mobile and the base station.

Fig. 9 shows the normalized maximum range versus the number of antenna elements for phased (with the IS-95 CDMA system model) and adaptive arrays with $\lambda/2$ antenna spacing and a three-finger RAKE receiver. As in Fig. 6, results are shown for different fixed scattering radii, with the scattering angle for the baseline case of one antenna element given. However, in Fig. 9 the baseline case includes a three-finger RAKE with its 6.8-dB diversity gain. Thus, the actual range in the baseline case is 1.48 $(= 10^{6.8/40})$ times greater than in Fig. 6. We also show the theoretical range increase due to antenna gain $(M^{1/4})$ and due to antenna gain and $3M$-fold diversity (versus three-fold diversity due to the RAKE receiver).

With the phased array and a single beam pointed at the mobile, the range limitation is similar to that of the narrowband system (Fig. 6). However, with a separate beam for each RAKE finger, Fig. 9 shows that the range limitation is negligible for scattering angles less than 20°, but there is

degradation in the range increase for scattering angles of 45° and 60° with more than about 40 antennas. This degradation is somewhat larger when fixed sectorized antennas, rather than continuously adjustable phased array antennas, are used, as Fig. 9 shows for the case of a 60° scattering angle.

With the adaptive array, the range exceeds the theoretical range due to antenna gain and three-fold diversity, showing the additional diversity gain. Thus, there is a significant improvement with adaptive arrays for large scattering angles and large M. Furthermore, in all cases the diversity gain of adaptive arrays increases with larger spacing, as shown in Fig. 9 for 5λ spacing with scattering angles of 3° to 0°.

IV. Conclusions

In this paper, we have compared the increase in range with multiple-antenna base stations using adaptive array combining to that of phased array combining. Our computer simulation considered a multipath model with a uniform distribution of scatterers within a given radius around the mobile, and determined the increase in range with arrays for 10^{-2} average BER with coherent detection of PSK. From our results we make the following conclusions.

- Phased arrays were shown to have a range increase limitation given by the scattering angle. For scattering angles of a few tenths of a degree (typical in rural areas), this limitation is significant only for arrays with more than 100 elements, while with larger scattering angles (typical in suburban and urban areas), the range increase limitation can occur with far fewer elements.
- For spread-spectrum systems, using a RAKE receiver with phased arrays, the maximum range increase degradation was much less than that of narrow-band systems.
- In both narrow-band and spread-spectrum systems, adaptive arrays had no range limitation and could achieve diversity gain with $\lambda/2$ antenna spacing with sufficiently many elements. Almost full diversity gain could be achieved with large arrays with antenna spacings of only a few wavelengths for scattering angles as low as 1°.

Appendix A

A. Effect of Antenna Spacing on Mutual Coupling

With an M-element array, the maximum gain is M without mutual coupling. Because of mutual coupling, however, this gain will vary with antenna spacing. Specifically, this gain is given by the directivity, i.e., the ratio of the peak to average gain for a signal arriving with a flat wavefront [20]

$$D = \frac{\max_{\theta,\phi} |E(\theta,\phi)|^2}{\frac{1}{4\pi}\int_0^{\pi}\int_0^{2\pi} \sin\theta |E(\theta,\phi)|^2 \, d\theta \, d\phi} \tag{A-1}$$

where $E(\theta,\phi)$ is the voltage gain at elevation angle θ and azimuth angle ϕ.

For the base-station antennas, we will assume that the variation in gain with elevation angle is independent of azimuth, i.e.,

$$E(\theta,\phi) = E_e(\theta)A(\phi) \tag{A-2}$$

where $E_e(\theta)$ and $A(\phi)$ are the variation in gain with elevation angle and azimuth angle, respectively. Thus, from (A-1) and (A-2), the directivity is given by

$$D = \frac{|E_e(\theta_{\max})A(\phi_{\max})|^2}{\frac{1}{4\pi}\int_0^{\pi} \sin\theta |E_e(\theta)|^2 \, d\theta \int_0^{2\pi} |A(\phi)|^2 \, d\phi} \tag{A-3}$$

where $\theta_{\max}$ and $\phi_{\max}$ are the peak-gain elevation and azimuth angles, respectively. If we consider the typical base-station antenna with a very narrow elevation beamwidth, then the directivity can be expressed as

$$D \approx G_{el} \frac{|A(\phi_{\max})|^2}{\frac{1}{2\pi}\int_0^{2\pi} |A(\phi)|^2 \, d\phi} \tag{A-4}$$

where G_{el} is the gain due to the elevation beamwidth. Since we are interested in the effect of mutual coupling on the horizontal antenna spacing, we will set $G_{el} = 1$ for simplicity.

Now, the voltage gain for a signal arriving at angle ϕ onto an M-element array (using maximal ratio combining to maximize gain) is given by

$$A(\phi) = \left| \sum_{i=1}^{M} s_i(\phi) s_i^*(\phi_{\max} \right| \tag{A-5}$$

where $s_i(\phi)$ is the complex signal gain (with phase relative to the other antennas) at the ith antenna element. We have assumed that the elevation beamwidth is very narrow, so that waves arriving at angles far enough from the equator to affect the relative phase between elements have negligible effect in the directivity calculation. Thus, the directivity is given by

$$D = \frac{\sum_{i=1}^{M} |s_i(\phi_{\max}|^2}{\frac{1}{2\pi}\int_0^{2\pi} \left| \sum_{i=1}^{M} s_i(\phi) s_i^*(\phi_{\max}) \right|^2 d\phi}. \tag{A-6}$$

First consider a linear array of omnidirectional elements with narrow elevation beamwidth, as with a vertical colinear array of dipoles (VCAD). In this case, the complex element responses are given by

$$s_i(\phi) = e^{j(i-1)(2\pi d/\lambda)\sin\phi}, \qquad \text{for } i = 1, \cdots, M \tag{A-7}$$

where d is the element spacing and ϕ is the angle relative to broadside.

Fig. 10 shows the directivity versus antenna spacing for an M-element array with the desired angle of arrival at broadside, $\phi_{\max} = 0$. There are large fluctuations in directivity with antenna spacing (particularly at spacings which correspond to the onset of new grating lobes), showing substantial mutual coupling, with a spacing of λ having about half the gain in decibels of a spacing of $\lambda/2$.

For a cylindrical array of equally spaced VCAD's with radius r and element 1 at 0°, the complex receive signal response at the ith element for a signal arriving at angle ϕ

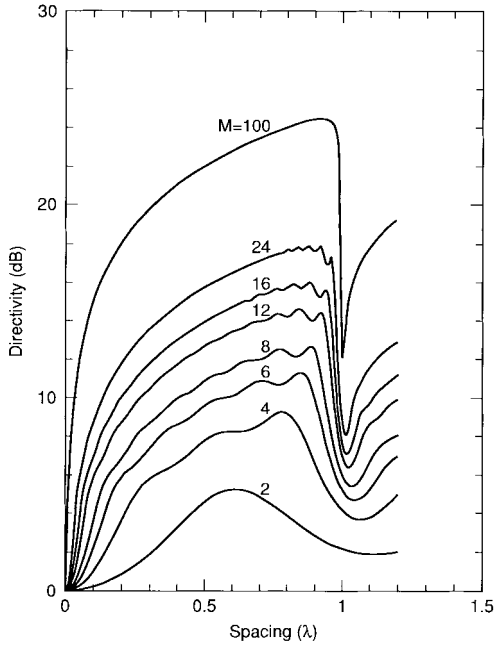

Fig. 10. Directivity versus antenna spacing for an M-element linear array with $\phi_{\max} = 0°$.

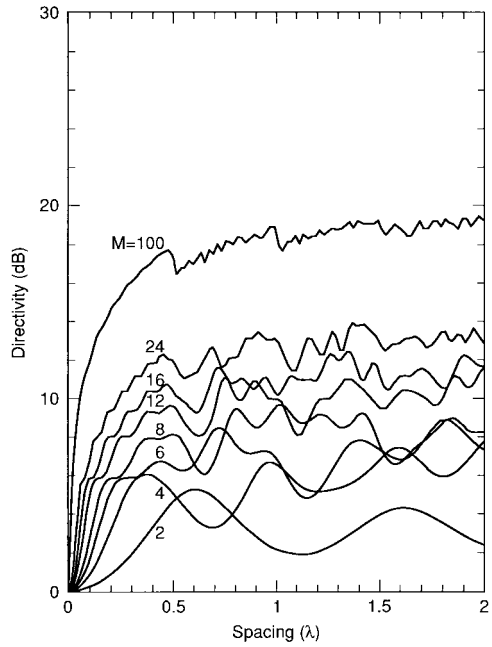

Fig. 11. Directivity versus antenna spacing for an M-element cylindrical array with dipole elements and $\phi_{\max} = 90°$.

is given by

$$s_i(\phi) = e^{j(2\pi r/\lambda)\cos[\phi-(2\pi(i-1)/M)]}, \qquad \text{for } i = 1, \cdots, M. \tag{A-8}$$

The spacing between adjacent elements is given by

$$d = 2r \sin \frac{\pi}{M}. \tag{A-9}$$

Fig. 11 shows the directivity versus antenna spacing for an M-element array with $\phi_{\max} = 90°$. Note that for spacings greater than $\lambda/2$, the gain variation with spacing is large for small M, but is less than 2 dB for $M = 100$. Thus, with the cylindrical array, the mutual coupling becomes much less than that of the linear array as M increases. This can be considered to be a result of adjacent elements being similar to endfire or broadside arrays, depending on their location around the circumference. Since grating lobes arise at different spacings for endfire than for broadside arrays, the mutual coupling fluctuations are somewhat reduced.

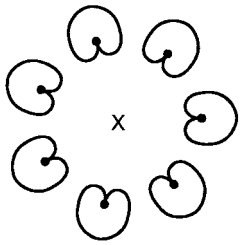

Fig. 12. Cylindrical array using cardioid-pattern antennas, with each element pointed away from the center of the array.

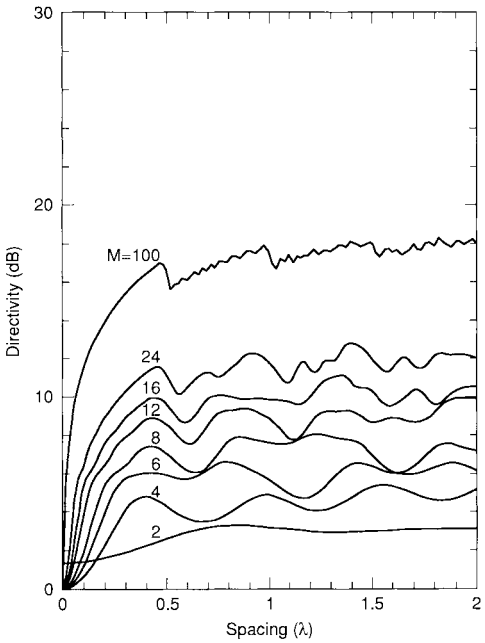

Fig. 13. Directivity versus antenna spacing for an M-element cylindrical array with cardioid elements and $\phi_{\max} = 90°$.

To decrease the mutual coupling for small M, consider the use of cardioid pattern antennas (with narrow elevation beamwidth), rather than VCAD's, with each element pointed away from the center of the array (see Fig. 12). With the cardioid antenna, the voltage gain for the ith element at angle ϕ is given by [20]

$$V_i(\phi) = \sqrt{2}\cos\Big(\frac{\pi}{4}(\cos[\phi - 2\pi(i-1)/M] - 1)\Big), \qquad \text{for } i = 1, \cdots, M. \tag{A10}$$

Fig. 13 shows the directivity versus antenna spacing for an M-element array with cardioid elements and $\phi_{\max} = 90°$. Note that for spacing greater than $\lambda/2$, the gain variation with spacing is greatly reduced with small M. Our results show

that the directivity variation is approximately the same for other values of $\phi_{\max}$ as well. Thus, with the cylindrical array of cardioid elements, the mutual coupling generates a gain variation of less than 2 dB for spacings greater than $\lambda/2$ for all values of M. We will therefore ignore the mutual coupling in our simulations and assume a gain of M.

ACKNOWLEDGMENT

It is a pleasure to acknowledge helpful suggestions by L. J. Greenstein.

REFERENCES

[1] S. C. Swales, M. A. Beach, D. J. Edwards, and J. P. McGeehan, "The performance enhancement of multibeam adaptive base-station antennas for cellular land mobile radio systems," *IEEE Trans. Veh. Technol.*, vol. 39, pp. 56–67, Feb. 1990.

[2] G. K. Chan, "Effects of sectorization on the spectrum efficiency of cellular radio systems," *IEEE Trans. Veh. Technol.*, vol. 41, pp. 217–225, Aug. 1992.

[3] J. C. Liberti and T. S. Rappaport, "Reverse channel performance improvements in CDMA cellular communication systems employing adaptive antennas," in *Proc. Globecom'93*, Houston, TX, Nov. 29–Dec. 2, 1993, pp. 42–47.

[4] S. P. Stapleton and G. S. Quon, "A cellular base station phased array antenna system," in *Proc. Veh. Technol. Conf.*, Secaucus, NJ, May 18–20, 1993, pp. 93–96.

[5] B. Khalaj, A. Paulraj, and T. Kailath, "Antenna arrays for CDMA systems with multipath," in *Proc. Milcom'93*, Boston, MA, pp. 624–628.

[6] A. F. Naguib and A. Paulraj, "Performance of CDMA cellular networks with base-station antenna arrays," in *Proc. Int. Zurich Seminar on Digital Communications*, Mar. 1994, pp. 87–100.

[7] J. H. Winters, "Optimum combining in digital mobile radio with cochannel interference," *IEEE J. Select. Areas Commun.*, vol. SAC-2, pp. 528–539, July 1984.

[8] ———, "Signal acquisition and tracking with adaptive arrays in the digital mobile radio system IS-54 with flat fading," *IEEE Trans. Veh. Technol.*, vol. 42, pp. 377–384, Nov. 1993.

[9] J. H. Winters, J. Salz, and R. D. Gitlin, "The impact of antenna diversity on the capacity of wireless communication systems," *IEEE Trans. Commun.*, vol. 42, no. 2/3/4, pp. 1740–1751, 1994.

[10] T. Ohgane, H. Sasaoka, N. Matsuzawa, K. Tekeda, and T. Shimura, "A development of GMSK/TDMA system with CMA adaptive array for land mobile communications," in *Proc. Veh. Technol. Conf.*, May 1991, pp. 172–177.

[11] "Smart antennas," Northern Telecom product brochure, 1992.

[12] W. C.-Y. Lee, "Effects on correlation between two mobile radio base-station antennas," *IEEE Trans. Commun.*, vol. COM-21, pp. 1214–1224, Nov. 1973.

[13] W. C. Jakes, Jr. *et al.*, *Microwave Mobile Communications*. New York: Wiley, 1974.

[14] Y. Yamada, K. Kagoshima, and K. Tsunekawa, "Diversity antennas for base and mobile stations in land mobile communication systems," *IEICE Trans.*, vol. E 74, pp. 3202–3209, Oct. 1991.

[15] M. Hata, "Empirical formula for propagation loss in land mobile radio," *IEEE Trans. Veh. Technol.*, vol. VT-29, pp. 317–335, Aug. 1980.

[16] J. Salz and J. H. Winters, "Effect of fading correlation on adaptive arrays in digital wireless communications," *IEEE Trans. Veh. Technol.*, vol. 43, pp. 1049–1057, Nov. 1994.

[17] R. Price and P. E. Green, "A communication technique for multipath channels," *Proc. IRE*, vol. 46, pp. 555–570, Mar. 1958.

[18] J. R. Treichler and B. G. Agee, "A new approach to multipath correction of constant modulus signals," *IEEE Trans. Acoust., Speech, Signal Process.*, vol. ASSP-31, pp. 459–472, Apr. 1983.

[19] R. A. Monzingo and T. W. Miller, *Introduction to Adaptive Arrays*. New York: Wiley, 1980.

[20] W. L. Stutzman and G. A. Thiele, *Antenna Theory and Design*. New York: 1981, pp. 115, 116, and 141.

Jack H. Winters (S'77–M'81–SM'88–F'96) received the B.S.E.E. degree from the University of Cincinnati, Cincinnati, OH, in 1977 and the M.S. and Ph.D. degrees in electrical engineering from Ohio State University, Columbus, in 1978 and 1981, respectively.

Since 1981, he has been with AT&T Bell Laboratories and now AT&T Labs–Research, where he is in the Wireless Systems Research Department. He has studied signal processing techniques for increasing the capacity and reducing signal distortion in fiber optic, mobile radio, and indoor radio systems and is currently studying adaptive arrays and equalization for indoor and mobile radio.

Dr. Winters is a member of Sigma Xi.

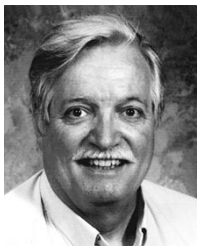

Michael J. Gans received the B.S. degree in electrical engineering from Notre Dame University, South Bend, IN, and the M.S. and Ph.D. degrees in electrical engineering from the University of California at Berkeley.

He is on the staff of the Wireless Communications Research Department, Bell Labs, Holmdel, NJ. He He has been at Bell Laboratories since 1966. His primary technical areas include mobile radio, antennas, satellites, fiber optics, and infrared communications.